

## Research Article

# Development of a New Aprepitant Liquisolid Formulation with the Aid of Artificial Neural Networks and Genetic Programming

Panagiotis Barmplexis,<sup>1,2,3</sup> Agni Grypioti,<sup>2</sup> Georgios K. Eleftheriadis,<sup>1</sup> and Dimitris G. Fatouros<sup>1</sup>

Received 9 July 2017; accepted 24 September 2017; published online 4 October 2017

**Abstract.** In the present study, liquisolid formulations were developed for improving dissolution profile of aprepitant (APT) in a solid dosage form. Experimental studies were complemented with artificial neural networks and genetic programming. Specifically, the type and concentration of liquid vehicle was evaluated through saturation-solubility studies, while the effect of the amount of viscosity increasing agent (HPMC), the type of wetting (Soluplus® vs. PVP) and solubilizing (Poloxamer®407 vs. Kolliphor®ELP) agents, and the ratio of solid coating (microcrystalline cellulose) to carrier (colloidal silicon dioxide) were evaluated based on *in vitro* drug release studies. The optimum liquisolid formulation exhibited improved dissolution characteristics compared to the marketed product Emend®. X-ray diffraction (XRD), scanning electron microscopy (SEM) and a novel method combining particle size analysis by dynamic light scattering (DLS) and HPLC, revealed that the increase in dissolution rate of APT in the optimum liquisolid formulation was due to the formation of stable APT nanocrystals. Differential scanning calorimetry (DSC) and attenuated total reflection FTIR spectroscopy (ATR-FTIR) revealed the presence of intermolecular interactions between APT and liquisolid formulation excipients. Multilinear regression analysis (MLR), artificial neural networks (ANNs), and genetic programming (GP) were used to correlate several formulation variables with dissolution profile parameters ( $Y_{15\text{min}}$  and  $Y_{30\text{min}}$ ) using a full factorial experimental design. Results showed increased correlation efficacy for ANNs and GP (RMSE of 0.151 and 0.273, respectively) compared to MLR (RMSE = 0.413).

**KEY WORDS:** aprepitant; liquisolid; solvent; poor solubility; release enhancement.

## INTRODUCTION

Aprepitant (APT) is a NK1 receptor antagonist used for the treatment of emesis associated with chemotherapy. It has little or no affinity for serotonin, dopamine, and corticosteroid receptors, the targets of existing therapies for chemotherapy-induced nausea and vomiting (CINV) (1). Currently, APT is available in several strengths (40, 80, 125, and 165 mg) manufactured by Merck Sharp & Dohme B.V. and commercially marketed under the tradename Emend® (2). APT's chemical name is 5-(((2R,3S)-2-((1R)-1-(3,5-

bis(trifluoromethyl)phenyl) ethoxy) -3-(4-fluorophenyl)-4-morpholinyl) methyl)-1,2-dihydro-3H-1,2,4-triazol-3-one, while its 2D chemical structure is given in SI (Fig. S1). It is a white to off-white crystalline solid powder sparingly soluble in ethanol and isopropyl acetate, slightly soluble in acetonitrile and practically insoluble in water. This low aqueous solubility of APT is the rate-limiting step for API's poor gastrointestinal absorption (3).

During the past decades, several techniques have been developed in an attempt to improve the bioavailability of poor aqueous solubility APIs. Such approaches include pro-drug and salt formation, particle size reduction (at micro- or nano- scale), solid dispersions, inclusion of liquid formulations into soft gelatin capsules, preparation of lipid-based formulations, self-emulsifying drug delivery systems, etc. (4). Among the others, APT has been successfully co-formulated, with microemulsions (5,6), solid dispersions (7–10), films (11), cyclodextrin complexes (12), and nanoparticles (3,13), however APT dissolution and bioavailability characteristic are hampered owing to the physicochemical characteristic of the API.

APT is characterized as a hydrophobic compound with logP 1.1, measured at  $25 \pm 2^\circ\text{C}$  1:1 n-octanol: water at pH 7.4

**Electronic supplementary material** The online version of this article (<https://doi.org/10.1208/s12249-017-0893-z>) contains supplementary material, which is available to authorized users.

<sup>1</sup>Department of Pharmaceutical Technology, School of Pharmacy, Aristotle University of Thessaloniki, 54124, Thessaloniki, Greece.

<sup>2</sup>Pharmaceutical RnD department, Rontis Hellas S.A., Maroussi, 15125, Athens, Greece.

<sup>3</sup>To whom correspondence should be addressed. (e-mail: panagiotis.barmplexis@rontis.com)

as per USP (shake flask method) and melting point of approximately 253°C (14). These characteristics categorize APT as a “brick dust” molecule, and hence the aqueous solubility of the compounds is restricted due to the presence of strong intermolecular bonds within the crystal structure. Generally, “brick dust” molecules, such as APT, are practically insoluble either in aqueous or oily media (15). In such cases, the development of micro- or nanonized formulation is the first choice of industrial production as in the case of the innovator product Emend®, which uses nanonization for the formulation of the commercially available APT (16).

Another promising approach for the dissolution enhancement of APT is the preparation of liquid oral formulations where the API is completely solubilized or dispersed in suitable medium carriers as stable nanoparticles. Wu *et al.* (3) showed that APT encapsulated in soft gelatin capsules exhibited remarkable increase in bioavailability when tested *in vivo*. However, such formulation approach would require at least ten (10) such capsules in a single dose when tested in humans. In addition, manufacturing of soft gelatin capsules is an expensive technique which requires sophisticated and specialized technology. One way in order to overcome both limitations is the absorption of the liquid formulation onto solid surfaces which have high specific surface area (liquisolid approach), which in turn enables free flowing, compressible powder which can be further formulated in the form of compacts either as tablets or capsules (17).

Liquisolid technique is a novel approach where a liquid formulation (in which the API is solubilized/suspended/emulsified in a suitable water-miscible nonvolatile solvent systems) is transformed into a free flowing, non-adherent, and readily compressible dry powder by applying a simple admixing of the liquid vehicle with selected carriers and coating materials. Compared to traditional wet granulation or solid dispersion techniques, in the case of liquisolid preparations, the solvent used during manufacturing process is not removed from the final dosage form, but is absorbed from selected solid carriers and coating materials. In this case, the increased surface area and the improved wetting properties of the API could lead to dissolution rate and bioavailability enhancement (18–23). Suitable liquid vehicles may include water-miscible liquids with high boiling point (and low vapor pressure), such as liquid polyethylene glycols, polysorbates, propylene glycol, or glycerin, while common excipients with high specific surface area, such as microcrystalline cellulose, lactose, starch, colloidal silicon dioxide, etc., may be used as solid carriers. In addition, several additives may be used in order to enhance further the dissolution rate of the API in the final formulation, or to improve its storage stability, such as disintegrants, solubilizers, wetting/amorphization agents, and moisture-absorbing agent (24–28).

To the best of our knowledge, this is the first enrolling liquisolid technology as a mean to increase APT dissolution rate. For this purpose, several liquid vehicles and solid additives were evaluated with the aid of artificial neural networks (ANNs) and genetic programming (GP). Microcrystalline cellulose and colloidal silicon dioxide used as suitable carrier and coating, respectively; while the optimum liquisolid formulation was compared to the innovator market product EMEND®.

## MATERIALS AND METHODS

### Materials

Micronized APT with purity 99.6% and d(90) of 13.8 μm (measured with Mastersizer 3000, Malvern, UK), as well as APT pure form I and II crystals were obtained from Jubilant (Jubilant Generics Limited, Karnataka, India). PEG 400 (Polyglykol400®, Clariant, Muttenz, Switzerland), poloxamer (Kollisolv®P124, BASF, Ludwigshafen, Germany), 2-pyrrolidone (Kollisolv®PYR, BASF, Ludwigshafen, Germany), propylene glycol (Kollisolv®PG, BASF, Ludwigshafen, Germany), medium chain triglycerides (Miglyol®810 N, Peter Cremer GmbH, Hamburg, Deutschland), caprylic-capric-succinic triglyceride (Miglyol®829, Peter Cremer, Hamburg, Deutschland), and glyceryl tricaprilate/tricaprate (Camptex®300, Abitec, Ohio, USA), tested as suitable liquid vehicles, were given as free samples from suppliers. Microcrystalline cellulose (Avicel®PH102) (FMC Corp., Philadelphia, USA), colloidal silicon dioxide (Aerosil300®, Evonik Industries AG, Essen, Germany), sodium lauryl sulfate (Kolliphor®SLS, BASF Ludwigshafen, Germany), poloxamer 407 (Kolliphor®P407, BASF, Ludwigshafen, Germany), hydroxypropyl methylcellulose (HPMC, Methocel®E4M, Colorcon, Dartford, UK), polyethylene glycol/polyvinyl acetate /polyvinyl-caprolactame based graft copolymer (Soluplus®, BASF, Ludwigshafen, Germany), povidone (Kollidon® K29/32, BASF, Ludwigshafen, Germany), crospovidone (Kollidon®CL-F, BASF, Ludwigshafen, Germany), and polyoxyl 35 hydrogenated castor oil (Kolliphor®ELP, BASF, Ludwigshafen, Germany), given as free samples from suppliers, were tested as carriers, coatings, and additives. Innovator marketed product, Emend® 125 mg, was purchased from a local pharmacy store. All other materials and reagents were of either pharmacological grade or analytical grade.

### Pre-Formulation Studies

#### *Solubility Studies*

An array of different solvents was employed to investigate the saturation solubility of APT namely; PEG 400, Kollisolv®P124, Kollisolv®PYR, Kollisolv®PG, Miglyol®810 N, Miglyol®829, Camptex®300, Acetone and Acetone-SLS mixtures. Specifically, excess amount of APT was added in 10 mL of the tested liquid solvents to produce saturated fractions of the API. The mixtures were remained under stirring for up to 72 h and then centrifuged at 6000 rpm for 10 min. The supernatants were filtered through PVDF filter (0.45 μm) and aliquots of either 15 or 25 μL were withdrawn and further diluted up to 1500 μL before analyzing for drug content.

#### *Determination of Optimal Flowable Liquid-Retention Potential ( $\varphi$ -Value) and Liquid Load Factor (Lf)*

The optimal flowable liquid-retention potential ( $\varphi$ -value) of a powder is the maximum amount of a given nonvolatile liquid that can be retained inside powder bulk ( $w/w$ ) while maintaining acceptable flowability. For the determination of  $\varphi$ -value, 5 g of each excipient was mixed with increasing

amounts of liquid vehicle using a mortar and pestle, and paced on a polished metal plate. The plate is tilted gradually until the admixture starts to slide. The angle of the plate formed during the slide is defined as the angle of slide and the  $\varphi$ -value is calculated based on the following equation (Eq. 1):

$$(\varphi\text{-value}) = (\text{weight of liquid vehicle}/\text{weight of solid}) \quad (1)$$

The optimum weight of solid content was calculated by plotting the calculated  $\varphi$ -value vs. the corresponding angle of the slide.  $\varphi$ -values close to approximately  $33^\circ$  represents the optimal flowable liquid-retention potential ( $\varphi$ -value) of the powder excipient in the corresponding liquid vehicle.

The liquid load factor (Lf) which is defined as the weight ratio of the liquid medication was determined by the API solubility studies (W) to carrier (Q) in the system (Eq. 2):

$$\text{Lf} = W/Q \quad (2)$$

The ratio (R) between the amount of carrier (Q) and coating (q) materials used in a liquisolid system is closely related to Lf based on the following equation (Eq. 3):

$$\text{L}_f = \varphi_{CA} + \varphi_{CO} (1/R) \quad (3)$$

where,  $\varphi_{CA}$  and  $\varphi_{CO}$  are the optimal flowable liquid-retention potential of the carrier and the coating materials, respectively.

### Preparation of Liquisolid Formulations

The  $\varphi$ -values obtained from the angle of slide were used for the calculation of Lf and the required amounts for carrier (Q) and coating (q) materials in each formulation were calculated according to these values ( $\varphi$  and Lf). Based on the calculated values the liquisolid formulation were prepared according to Spireas & Bolton (17). Each liquisolid formulation contained 1 g of API and the amount of liquid medication (W) required in order to fully solubilize the API. The effect of the amount of the viscosity increasing agent (HMPC) and the type of wetting agents (Soluplus and PVP) on dissolution profile (both added into the API solution) was evaluated using an OFAT approach (One Factor at Time, Table I), whereas the carrier/coating ratio ( $X_1$ :  $R = Q/q$ ) and the type of solubilizing agents ( $X_2$ : Poloxamer®407 and Kolliphor®ELP) were evaluated with the aid of a full factorial design (Table II). The percent amount of API dissolved in 10 min ( $Y_1$ ) and 30 min ( $Y_2$ ) were selected as response factors. The DesignExpert® software package (vs.6.0.4, Stat-Ease Inc., Minneapolis, MN) was used for the preparation and evaluation of the selected experiment design. A multilinear regression model (MLR) was used in order to estimate the main and two-way interactions effects (Eq. 4):

$$Y_i = b_0 + b_1X_1 + b_2X_2 + b_{12}X_1X_2 \quad (4)$$

where  $Y_i$  is the measured response,  $b_0$  is an intercept term,  $b_i$  to  $b_{ij}$  are regression coefficients for the main effects and two-way interaction, respectively, and  $X_i$  is the coded levels of formulation factors.

**Table I.** Formulation trials for evaluation of amount viscosity increasing agent (HMPC) and type of wetting agent (Soluplus® vs. PVP)

Code	Viscosity increasing agent, (mg/capsule)	Type of wetting agent
F1	0	Soluplus®
F2	20	Soluplus®
F3	40	Soluplus®
F4	20	PVP

All formulations were mixed with 7% of croscopvidone in a bi-cone blender (12 rpm, 10 min) and then lubricated with 3% SLS (12 rpm, 3 min). Hard gelatin capsules containing 80 and 125 mg of APT were filled using a hand-held capsule filling system (Profiller 1100, Torpac, NJ, USA). In all formulation trials, a stable final net weight was maintained (600 and 937.5 mg for 80 and 125 mg API, respectively), while MCC was used (mixed along croscopvidone) in order compensate for changes in capsule weight during composition evaluation experiments (F1-F8, Tables I and II).

### HPLC Analysis

The actual drug content of the prepared hard gelatin capsules and Emend® (100.3%) was assayed using the following validated isocratic HPLC method. A Waters 2695 HPLC system (WATERS, Massachusetts, US) consisting of a degasser, a pump, an auto sampler, a UV-Vis detector, and a column oven was used. Chromatographic analysis was performed on an XTerra RP-8 column (150 × 4.6 mm, 5  $\mu$ m). The mobile phase used was buffer pH 4.00/ acetonitrile (50:50 v/v) with a flow rate of 1.0 mL/min, and the column temperature was 30°C. Injection volume was set at 20  $\mu$ L, and APT was detected at 210 nm. All excipients used in the present study did not interfere with the assay of APT.

### In vitro Dissolution Studies

*In vitro* release of APT was evaluated using USP XXXII dissolution apparatus II on an Agilent 708-DS (Agilent Technologies LDA UK Limited, Cheshire, UK). The dissolution medium consisted of 500 mL 0.1 N HCl with the addition of 0.5% SLS. The test was performed at  $37 \pm 0.5^\circ\text{C}$  under stirring at 50 rpm. Sink conditions were maintained throughout the test.

**Table II.** Experimental domain and results according to the full factorial design applied in the study along with innovator product Emend® ( $X_1$ : carrier/coating ratio,  $X_2$ : type of solubilizing agents,  $Y_{10\text{min}}$ : %API dissolved in 10 min and  $Y_{30\text{min}}$ : %API dissolved in 30 min)

Code	Independent variables		Responses	
	$X_1$	$X_2$	$Y_{10\text{min}}$	$Y_{30\text{min}}$
F5	2/1	Poloxamer®407	31.1	61.6
F6	2/1	Kolliphor®ELP	17.1	39.4
F7	5/1	Poloxamer®407	36.9	70.9
F8	5/1	Kolliphor®ELP	26.3	59.0

The prepared and commercial capsules at an equivalent dose of 125 mg APT were placed into the dissolution tester and at pre-determined intervals (5, 10, 15, 20, 30, 45, and 60 min), 4 mL of the medium was sampled an automatic sampler (Agilent 850-DS sampling station) and filtered through a membrane filter (0.1  $\mu\text{m}$ ). The concentration of APT in the filtrate was analysed by HPLC using the apparatus and methodology mentioned above. Each test was performed in triplicate.

## Symbolic Regression

### *Artificial Neural Networks (ANNs)*

A feed-forward back-propagation ANN with a logistic sigmoid activation function was employed. All data derived from the factorial design (both input and output) were scaled from 0 to 1 and then split into two subsets (training and validation) based on the Kennard–Stone design or “uniform mapping algorithm” (29). ANN’s optimum structure and level of iterating cycles was identified by preliminary trial-and-error tests. Briefly, a single hidden layer was employed and networks having 2–8 hidden units were trained at 1000 iterating cycles, until the minimum RMSE of calibration was achieved. Then, the network was trained with 500–5000 iterating cycles in order to identify the optimum number of iterations. Scaled conjugate gradient (scg) descent method was employed in all network training and the “early stopping” method was used to avoid over-fitting. All networks were prepared and trained with the aid of Netlab Toolbox on Matlab v.7.0 R14 software program (Mathworks Inc.).

### *Genetic Programming (GP)*

GP automatically generates fitting equations in order to ‘naturally’ select those that give the best solution to an investigated problem. The evolutionary process based Darwin’s natural selection theory generates a random population (fitting equation), and then, by applying basic genetic operations such as “reproduction,” “crossover,” and “mutation” creates new populations (fitting equation) until a close data fitting is achieved (30,31). The efficiency of the process is determined by a set of parameters (such as crossover rate, mutation rate, population size, tournament size) that control the way in which the search for the ideal solution is conducted. Optimum population size was 500 (with 100 generation), crossover rate was set at 0.85, mutation at 0.1, reproduction at 0.05, while “times,” “minus,” “plus,” “divide,” “sqroot,” “log,” “square,” “sin,” “sinh,” “cos,” “cosh,” “tan,” “tanh,” and “exp” were set as functions. Constant range was between – 10 to 10 by 0.001 with a probability of 0.3 and elitism was set at 0.05. Tournament size was set at 3 while the root mean squared error (RMSE) was used as fitness function. All GP fitting was conducted using GPTIPS Toolbox on Matlab v.7.0 R14 software program (Mathworks Inc.).

## Physicochemical Characterization

### *Powder X-Ray Diffraction (XRD)*

XRD patterns of the raw material and the optimum formulations was measured on a Bruker D2 Phaser powder diffractometer with a nickel-filtered radiation. The patterns

were recorded on a quartz plate at a tube voltage of 30 kV and a current of 10 mA applying a scan rate of  $0.02^\circ 2\theta/\text{s}$  in the angular range of  $5\text{--}45^\circ 2\theta$ . The accuracy of the instrument was tested against a corundum A26-B29-S reference sample.

### *Novel PSD Analysis with Dynamic Light Scattering (DLS) and HPLC*

Dynamic light scattering (DLS) measurements were performed in a Malvern Nanosizer ZS, (Malvern Instruments, UK), equipped with a 4 mW He-Ne laser, operating at a wavelength of 633 nm and having an avalanche photodiode as a detector. In DLS, the scattered light is measured at an angle of  $173^\circ$ . Reported polydispersity index (PdI) values, ranging from 0 for an ideally monodispersed sample to 1 for very large size distributions, derive from the formula  $\text{PdI} = \sigma^2/\text{Dh}^2$ , where  $\sigma$  is the standard deviation of the distribution (nm) and Dh is the volume-weighted mean hydrodynamic diameter.

For the determination of APT particle size distribution in the prepared liquisolid formulations a novel combination of DLS and HPLC analysis was employed. Analytically, samples of 20 mg (prior to mixing with crospovidone and lubricating with SLS) were dissolved in 80 mL of purified water under stirring at 400 rpm for 6 h in order to remove all water-soluble and water-miscible excipients. In order to ensure that APT is not solubilized in the resultant mixture of water with all water-soluble and water-miscible excipients, the solubility of the API after 6 h of stirring was measured (a sample was withdrawn, filtered with 0.1  $\mu\text{m}$  filter and analyzed using the above HPLC method) and found to be negligible (below 0.2%). The resulting suspension was centrifuged at 4000 rpm for 30 min with the addition of hydrofluoric acid in order to dissolve the colloidal silicon dioxide. The resultant sediment was dissolved in copper tetrammine in order to remove MCC and further centrifuged at 5600 rpm for 30 min. The resultant sediments were re-dispersed in purified water and analyzed sequentially by DLS for particle size and HPLC for drug content determination. APT solubility in all used solvents during the above sample treatment was negligible.

### *Scanning Electron Microscopy (SEM)*

The morphology of the optimum formulation (prior to mixing with crospovidone and lubricating with SLS) was examined by a scanning electron microscopy system (SEM) JEOL JMS-840A. The samples were covered with carbon coating in order to increase conductivity of the electron beam. Operating conditions were accelerating voltage 20 kV, probe current 45 nA, and counting time 60 s.

### *Differential Scanning Calorimetry (DSC)*

DSC for the starting materials and the optimum prepared formulation were obtained using with the aid of a DSC 204 F1 Phoenix heat-flux differential scanning calorimeter (NETZSCH, Germany). Accurately weighted amounts of samples (3–5 mg) were placed in perforated aluminum pans and scanned through a temperature range of  $20\text{--}300^\circ\text{C}$  at a heating rate of  $10^\circ\text{C}/\text{min}$ , under a nitrogen purge gas flow of 70 mL/min. The instrument was calibrated for temperature and energy using indium standards. For determination of



APT glass-forming-ability (GFA), pure APT was heated from 25 to 5°C above the melting temperature, and held isothermally for 5 min to ensure complete melting. The sample was then cooled to -50°C and held for 15 min. Finally, the sample was heated again to 20°C above the melting temperature. A constant heating and cooling rate of 10°C/min was used.

#### Attenuated Total Reflection-FTIR Spectroscopy

FTIR spectra in the region of 500–4000 cm<sup>-1</sup> for the starting materials and the optimum prepared formulation were obtained using a Shimadzu IR-Prestige-21 FTIR spectrometer coupled with a horizontal Golden Gate MKII single-reflection ATR system (Specac, Kent, UK) equipped with a ZnSe lense after appropriate background subtraction. Sixty four scans over the selected wave number range at a resolution of 4 cm<sup>-1</sup> were averaged for each sample.

## RESULTS

### Solubility of APT in Various Liquid Vehicles

Saturated solubility results showed that APT exhibits poor solubility in all tested media except Kollisolv®PYP. Analytically, APT solubility in Miglyol®810 N, Miglyol®829 and Campdex®300 was below 1 mg/mL; whereas for PEG-400, Kollisolv®PG and Kollisolv®P124 API's solubility was 12.61, 6.87, and 2.68 mg/mL, respectively. The best results in terms of solubility were observed for Kollisolv®PYP where API's solubility was 249.55 mg/mL.

### Flowable Liquid-Retention Potential ( $\varphi$ -Value) and Liquid Load Factor (Lf)

Figure I shows the relationship between the angle of slide and the corresponding  $\varphi_{CA}$ -value (MCC) and  $\varphi_{CO}$ -value (Aerosil) for Kollisolv®PYP. Results indicated that the flowable liquid-retention potential for carrier ( $\varphi_{CA}$ ) and coating ( $\varphi_{CO}$ ) was 0.8 and 1.0, respectively; while the liquid load factor (Lf), calculated on Eq. 3 for two R values (5/1 and 2/1) was 1.0 and 1.3, respectively.

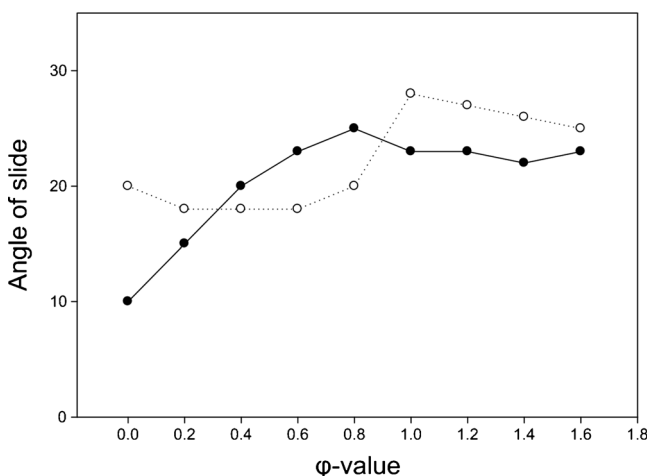


**Fig. I.** Angle of slide of various mixtures of powder MCC (●) and Aerosil (○) with Kollisolv®PYP. The  $\varphi$ -value which corresponds to an angle of slide close to 33° was chosen as optimum

### In vitro Dissolution Studies

The dissolution profiles of liquid formulations having different amounts of HPMC are illustrated at Fig. IIa. Results indicated that increasing amounts of HPMC from zero (F1) to 20 mg (F2) leads to increasing API's dissolution rate; whereas a further increase of HPMC to 40 mg (F3) shows a reduction in dissolution. Moreover, the presence of different types of wetting agents affected the dissolution profiles of formulations. Results showed that in the case of PVP (F4) a reduction in API's dissolution rate was observed compared to Soluplus® (F2).

Figure IIb depicts the dissolution profiles of the innovator product Emend® and the liquid formulations based on the selected experimental design (Table II). Results showed increased dissolution rates in all liquid formulations compared to the innovator congener product (Emend®), with the exception of formulation F6 where the carrier to coating ratio was 2/1 and Kolliphor®ELP was used as solubilizer.

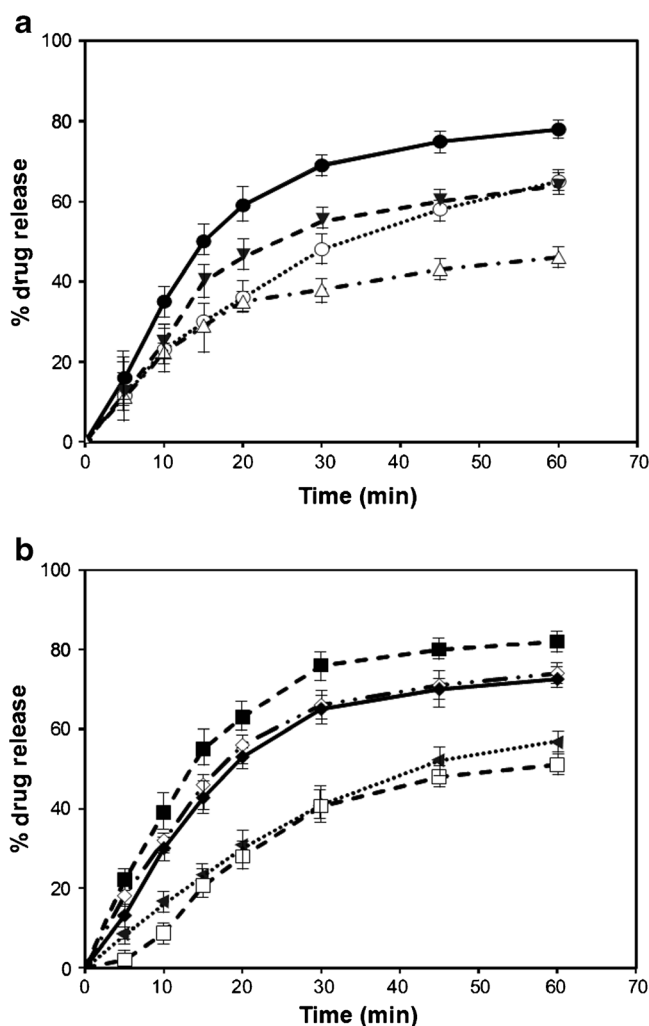


**Fig. II.** Aprepitant dissolution profile from tested liquid formulations (F1 (○), F2 (●), F3 (▼), F4 (△), F5 (◆), F6 (▲), F7 (◇), and F8 (□)) and innovator product Emend® (□) ( $n = 6$ )

### Physicochemical Characterization of the Optimum Liquisolid Formulation

The XRD patterns of the APT form I and II crystals, the API used in the study, the innovator product Emend®, the optimum liquidsolid formulation, and the relevant placebos are shown in Fig. III. Concerning the two polymorphs, main reflection peaks were identified in 12.1°, 15.3°, 17.7°, 19.5°, 20.7°, and 24.7° for form I and 15.3°, 17.5°, 20.5°, and 24.7° for form II. The XRD pattern of APT revealed that the API used in the present study was crystal with characteristic reflection peaks at 8.2°, 12.2°, 16.1°, 17.1°, 20.7°, 22.8°, 24.3°, 24.8°, and 26.6°. In addition, the XRD patterns of innovator product, Emend®, and the optimum liquidsolid formulation revealed the presence of APT crystals.

Figure IV shows a SEM micrograph of the optimum formulation. Based on the image, small irregularities in the range of 150–300 nm were identified on the surface of the sample.

Figure V shows the DSC thermograms of the pure APT, the optimum liquidsolid formulation, and the excipients used during manufacturing process. APT showed a sharp endothermic peak at 256.7°C (melting point); Soluplus showed a glass transition temperature ( $T_g$ ) at 74.3°C; SLS showed an initial endothermic peak at 116.3°C (dehydration process) and a melting peak at 206.7°C, followed by several decomposition phenomena; Kolliphor® PYR showed a boiling peak at 259.5°C; Poloxamer®407 showed a melting peak at 59.1°C; MCC showed a broad endothermic peak at 100°C; while HPMC and Aerosil®300 showed no thermal events. Optimum liquidsolid formulation showed a melting peak at 39.9°C and two broad endothermic peaks at 110.7 and 242.3°C. The DSC thermographs of the heating-cooling-heating cycle of pure API (supplemental 1) showed a melting point at 256.7°C during the first heating scan, a  $T_g$  at 91.5°C, a crystallization

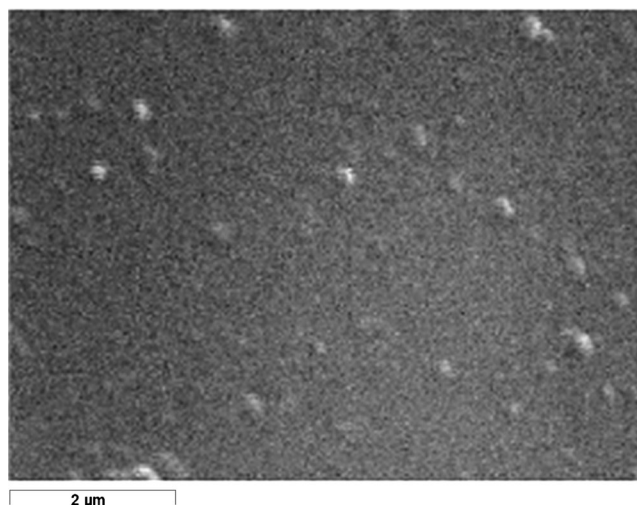


Fig. IV. SEM micrograph of the optimum liquidsolid formulation

exotherm at 167.7°C, and a melting peak at 248.5°C during the second heating scan, while no thermal events were recorded during cooling scan.

Figure VI shows the ATR-FTIR spectra of the pure APT, the optimum liquidsolid formulation, and the excipients used during manufacturing process in the region of 800–1500  $\text{cm}^{-1}$  where several FTIR peaks are recorded corresponding to the functional groups of each material.

### Multivariate Analysis

#### Multilinear Regression (MLR)

Regarding the multivariate linear regression analysis, adequate precision (depicts the value of signal to noise ratio;

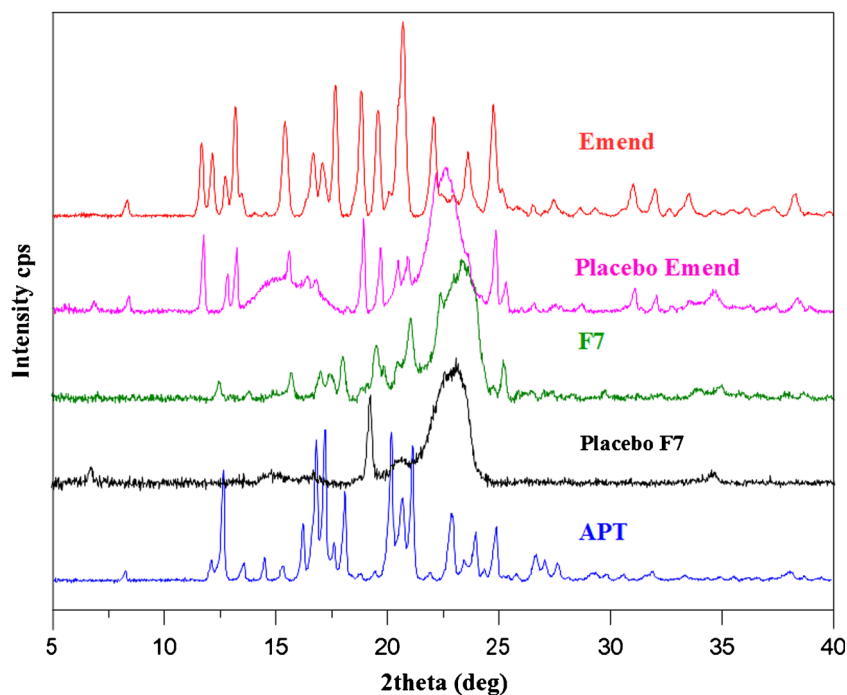
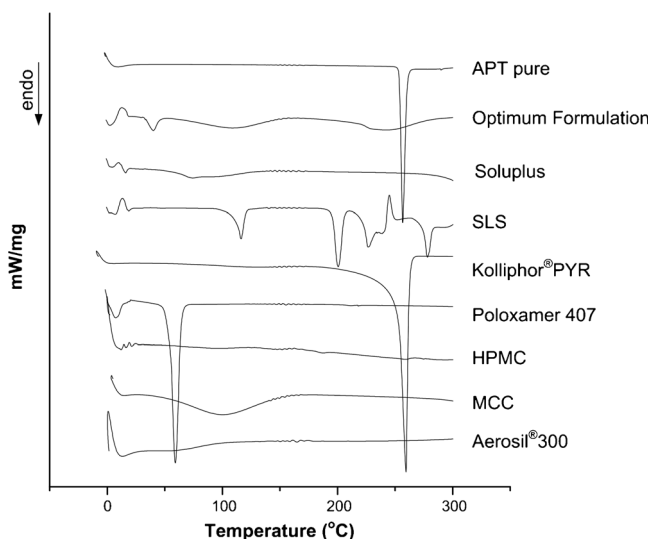


Fig. III. Powder XRD patterns of pure aprepitant (APT), innovator product (Emend®), optimum liquidsolid formulation (F7), and placebos



**Fig. V.** DSC thermograms of pure APT, optimum liquisolid formulation, and the excipients used during manufacturing process

ratio greater than 4 is preferred), coefficient of variation (CV) (measures the reproducibility of the model; a value less than 10% is desirable), and  $p$  value of the model ( $p < 0.05$  is needed) were all in the desirable limits (adequate precision = 12.44 and 15.13, CV = 8.33 and 6.01%, and model  $p$  value  $< 0.0001$  for response factors  $Y_{10\text{min}}$  and  $Y_{30\text{min}}$ , respectively). The calculated ANOVA  $F$  values for  $X_1$ ,  $X_2$

and  $X_3$  were 50.04, 67.96, and 7.58, respectively, while in all cases  $p$  values were below 0.05. Hence, ANOVA analysis indicated that both factors ( $X_1$  and  $X_2$ ) had significant effect on the selected responses, while the interaction effect of  $X_1$  and  $X_2$  had a significant effect only on the late stage of APT's dissolution ( $Y_{30\text{min}}$ ).

At Fig. V, the main effect plots for both  $Y_{10\text{min}}$  and  $Y_{30\text{min}}$  are illustrated. Plot analysis showed that  $Y_{10\text{min}}$  and  $Y_{30\text{min}}$  values varied from 32.83 to 39.15% and 64.65 to 73.14% for carrier/coating ratio 2/1 and 5/1, respectively; whereas the same responses varied from 34.50 to 22.31% and 67.63 to 50.81% when Poloxamer®407 and Kolliphor®ELP were used as solubilizers, respectively. The developed MLR regression models after the removal of insignificant factor by a backward elimination process (alpha out = 0.05) for both response are (factors in coded form - 1 to 1)

$$Y_{10\text{min}} = 29.35 + 3.05X_1 - 6.86X_2 \quad (5)$$

$$Y_{30\text{min}} = 55.62 + 6.83X_1 - 8.13X_2 + 2.93X_1X_2 \quad (6)$$

#### Artificial Neural Networks (ANNs)

Figure VII shows the calculated RMSE values of ANN models during the evaluation of hidden units number (Fig. VIIa)

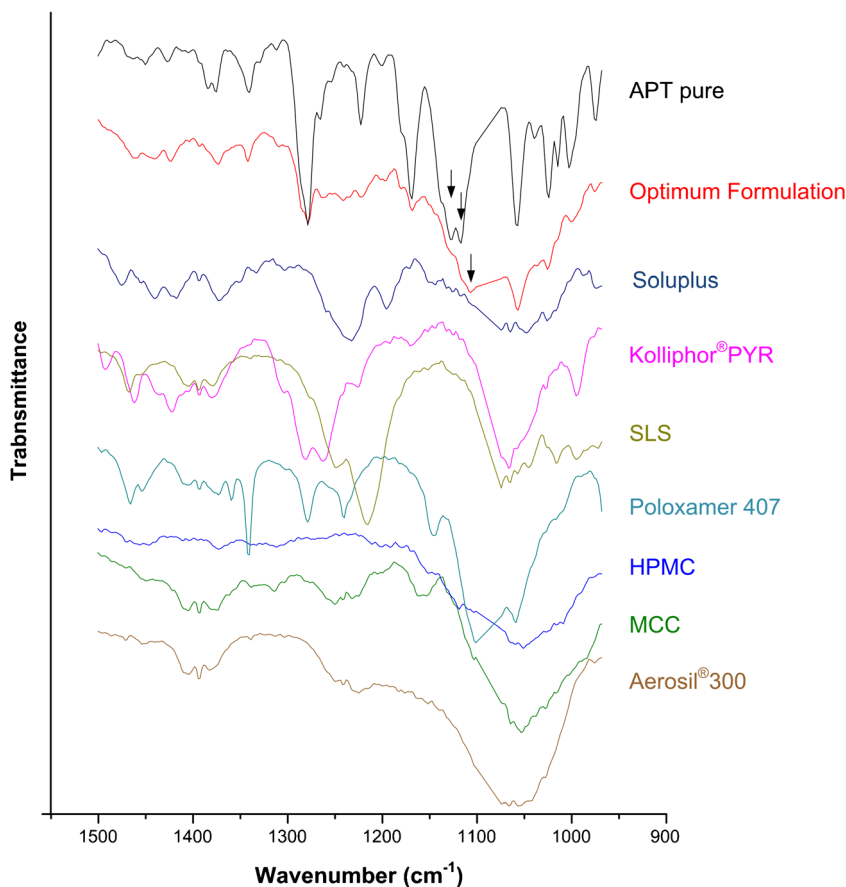


**Fig. VI.** ATR-FTIR spectra of pure APT, optimum liquisolid formulation, and the excipients used during manufacturing process

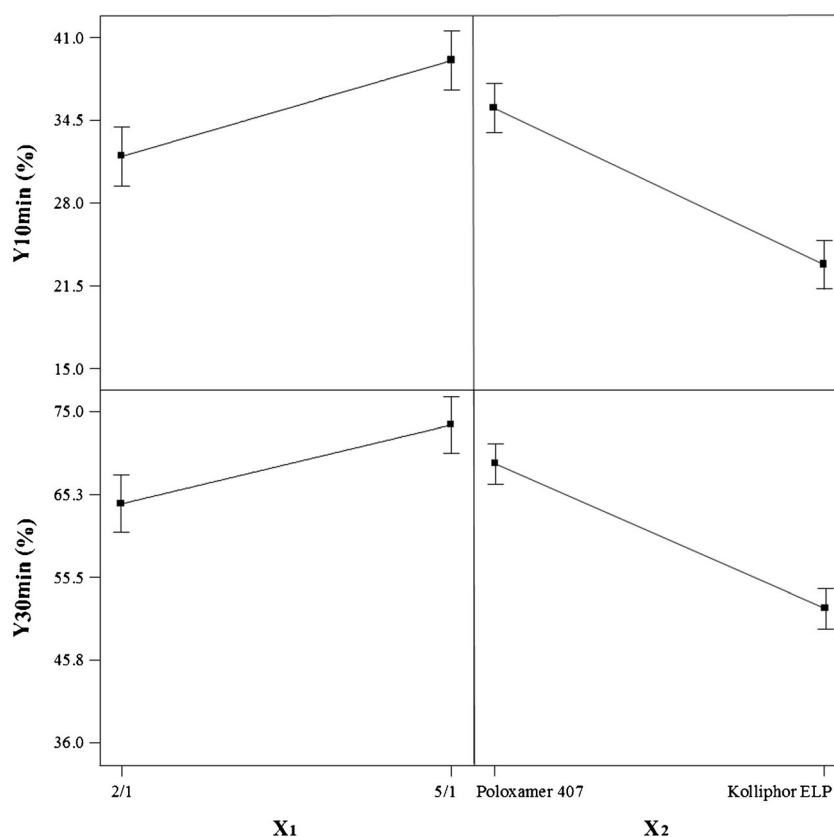


Fig. VII. Main effect plots for the proposed factorial design

and optimum iteration cycles (Fig. VIIb). RMSE values varied from 0.167 (for 2 hidden units) to 0.151 (for 4 hidden units) and 0.1514 (for 500 and 5000 iteration cycles) to 0.1512 (for 3000 iterations).

#### Genetic Programming (GP)

The application of symbolic regression by GP resulted in the following equations for the correlation of the formulation factors with the selected responses:

$$Y_{10\min} = 0.356 - 0.005X_1 + 0.071X_2 + 0.418\text{tanh}(X_1) \quad (7)$$

$$Y_{30\min} = 0.038 + (0.316X_2 - 0.023X_1) X_1 + 0.095\sin(X_2) \quad (8)$$

## DISCUSSION

### API's Solubility in Liquid Vehicles

Solubility studies revealed that Kolliphor®PYR is the most suitable solvent for APT. However, based on toxicity data, the maximum daily intake of 2-pyrrolidone should not exceed 144 mg (32). At this level, only a portion of the total APT dose could be fully solubilized and hence, a mix of acetone and aqueous solution of 5% w/w SLS (APT solubility = 123.1 mg/mL) was added in 2-pyrrolidone in order to fully solubilize the API. The excess amount of acetone/water was removed in a later stage with the aid of a fluid bed drier.

### In vitro Dissolution Studies

Dissolution profile analysis of liquisolid formulations having different amounts of viscosity agent HPMC E4M (Fig. IIa) showed an increase in API's dissolution rate when HPMC E4M content increased from zero (F1) to 20 mg (F2). This increase is probably caused due to API's increased dispersibility in the presence of HPMC E4M which leads to a higher exposed API's available surface area for solubilization. In general, HPMC, as other cellulose based polymers, interferes with one or both of API's precipitation (or re-crystallization) processes, viz. nucleation and crystal growth, leading to dissolution rate enhancement by forming fully (or partially) amorphous API dispersions or stable API nanocrystals (33). However, the further increase of HPMC E4M to 40 mg (F3) showed a reduction in dissolution rate, which might be attributed to the formation of an *in situ* gel-type matrix, which in turn delays the solubilization process of the API during dissolution. In addition, dissolution results showed a reduction in API's dissolution rate when PVP K29/32 was used as a wetting agent compared to Soluplus®, which may be attributed to the complete solubilization of Soluplus® in the liquid vehicle compared to PVP K29/32 where only a portion of the excipients was solubilized.

Furthermore, dissolution analysis of several liquisolid formulation showed increased dissolution rates compared to the innovator product (Fig. IIb). This enhancement in dissolution rates indicates that the selected liquisolid technique was able to increase significantly the dissolution rate of APT and most probably its bioavailability compared to the marketed product Emend®, where nanocrystals of the API are produced through



media milling. The optimum liquisolid formulation in terms of dissolution profile was F7, in which carrier to coating ratio was 5/1 and Poloxamer®407 was used as solubilizer.

### Physicochemical Characterization of the Optimum Liquisolid Formulation

Concerning the XRD pattern of the two polymorphs, characteristic reflection peaks especially in the region of 15–25°, show that each form contains unique reflections which can be used to confirm the presence of either pure form I or form II in the API (form II: 18.3 ° and 21.11°, form I: 15.6 °, 17.7 ° and 22.2 °). In addition, the XRD diffraction peaks of the pure API, coincide mainly with diffraction reflections of form II, while some additional minor peaks of form I were also recorded. XRD analysis of the innovator product, Emend®, and the optimum liquisolid formulation showed that in both cases the API remained in crystal form. In the case of Emend® pure APT, form I crystals were observed, while in the case of the prepared liquisolids a mixture of form II and I crystals was recorded. Furthermore, the XRD patterns of Fig. III show that the pattern of the new liquisolid formulation consists of peaks with lower reflection intensity compared to Emend®. These lower intensities may attributed to a partial amorphization of the API and the formation of nanocrystals within the matrix of the prepared formulation.

SEM analysis in Fig. IV showed a small irregularities in the range of 150–300 nm. These irregularities can be attributed to the formation of APT nanocrystals; however, the presence of pure excipient aggregates or a mixture of API and excipients at nanoscale cannot be excluded. Thus, in order to clarify the nature of the observed nanoparticles, PSD and drug content analysis after removal of all inactive ingredient/excipients was performed according to the method described in section 2.7.2 and 2.4, respectively. Results indicated that the nanoparticles had a z-average particle size of 200–300 nm, while HPLC analysis revealed the presence of pure (100%) APT in the examined nanoparticles.

Hence, based on the above analysis, the prepared liquisolid technique resulted in the formation of APT nanocrystals which were able to increase API's dissolution profile compared to the innovator product Emend®. In addition, stability studies conducted for the optimum liquisolid formulation revealed good storage stability in terms of dissolution profile and physicochemical characteristics (no amorphous/polymorphic transformations were observed) for up to six (6) months when stored at room temperature (data not shown).

DSC and ATR-FTIR analysis were used in order to identify any possible intermolecular interactions between the API and the selected excipients. Initially, the heating-cooling-heating DSC cycle for pure APT shown in supplemental 1, showed that the API can be categorized as a Class III non stable glass former that only recrystallizes during the second heating scan (34), indicating that the API is a good candidate for preparing amorphous based formulations (such as liquisolids). DSC thermogram of the optimum liquisolid formulation (Fig. V) showed an initial endothermic peak at 39.9°C (corresponding to the melting point of Poloxamer®407) and two broad endothermic peaks at 110.7 oC (due to MCC and

dehydration process) and 242.3°C, respectively. No clear API endothermic melting peak was recorded. This absence of a sharp API melting peak during DSC scanning, indicated that intermolecular interactions may be present between APT and the used excipients. In order to identify these interactions ATR-FTIR measurements were conducted (Fig. VI). Spectra analysis of the pure API and the optimum liquisolid formulation showed a shift to lower wavenumbers for the two FTIR peaks corresponding to the CF<sub>3</sub> group (35) of APT (arrows in the region of 1130 to 1160 cm<sup>-1</sup>), indicating that an intermolecular interaction is taking place among API's fluorine atoms and the functional groups of the selected liquisolid excipients. No other excipient FTIR peaks were recorder in the said area. Hence, based on the above analysis, the intermolecular interactions between the API and the selected excipients lead to partial API amorphization and stabilization of the prepared nanocrystals.

Finally, in order to evaluate the effect of SLS and crospovidone contents in APT dissolution profile, formulations containing 1% w/w of SLS and 4% w/w crospovidone, were prepared. Results (data not shown) revealed similar dissolution profiles (f2 similarity factor above 50 in all cases) compared to the initial optimum formulation where 3 and 7% of SLS and crospovidone were used, respectively, indicating that both materials do not affect APT's dissolution profile.

### Multivariate Analysis and Comparison

ANOVA analysis for MLR models, indicated that both factors ( $X_1$  and  $X_2$ ) had significant effect on the selected responses, while the interaction effect of  $X_1$  and  $X_2$  had a significant effect only on the late stage of APT's dissolution ( $Y_{30\text{min}}$ ). Main effect plot analysis for  $Y_{10\text{min}}$  and  $Y_{30\text{min}}$  (Fig. VII) revealed that as the coating to carrier ratio ( $X_1$ ) increases both  $Y_{10\text{min}}$  and  $Y_{30\text{min}}$  increase, whereas the use of Kolliphor®ELP instead of Poloxamer®407 as solubilizing agent ( $X_2$ ) leads to a reduction in both response factors. This difference may be attributed to the different physicochemical properties of both materials. Kolliphor®ELP is a nonionic emulsifying agent made by reacting castor oil with ethelene oxide in a molar ration of 1:35 followed by a purification process, with a hydrophilic-lipophilic balance (HLB) value of 13.9 (36), while Poloxamer®407 is nonionic polyoxyethylene-polyoxypropylene copolymer used primarily in pharmaceutical formulations as solubilizing agent with a HLB value of 22 (37). This increased hydrophilicity of Poloxamer®407 (expressed by the higher HLB value) might be responsible for the enhancement of APT dissolution from its liquisolid formulations compared to Kolliphor®ELP. However, as indicated in Eq. 6, there is a significant interaction between  $X_1$  and  $X_2$  showing a synergistic effect on  $Y_{30\text{min}}$  (positive sign in Eq. 6) meaning that the retardation of APT dissolution rate by the presence of Kolliphor®ELP is compensated by the presence of 5/1 carrier to coating ratio (F8 in Fig. IIB). The correlation coefficient values ( $R^2$ ) for MLR were 0.883 and 0.946, while the average RMSE of correlation was 0.413.

Regarding ANNs, RMSE plots in Fig. VIII showed that, as the number of hidden units and iteration cycles increases up to four for the number of hidden units and up to 3000 for the iterations, ANN training performance improves; whereas a further increase in the number of hidden units and iterations, leads to network over-fitting. Hence, the optimum

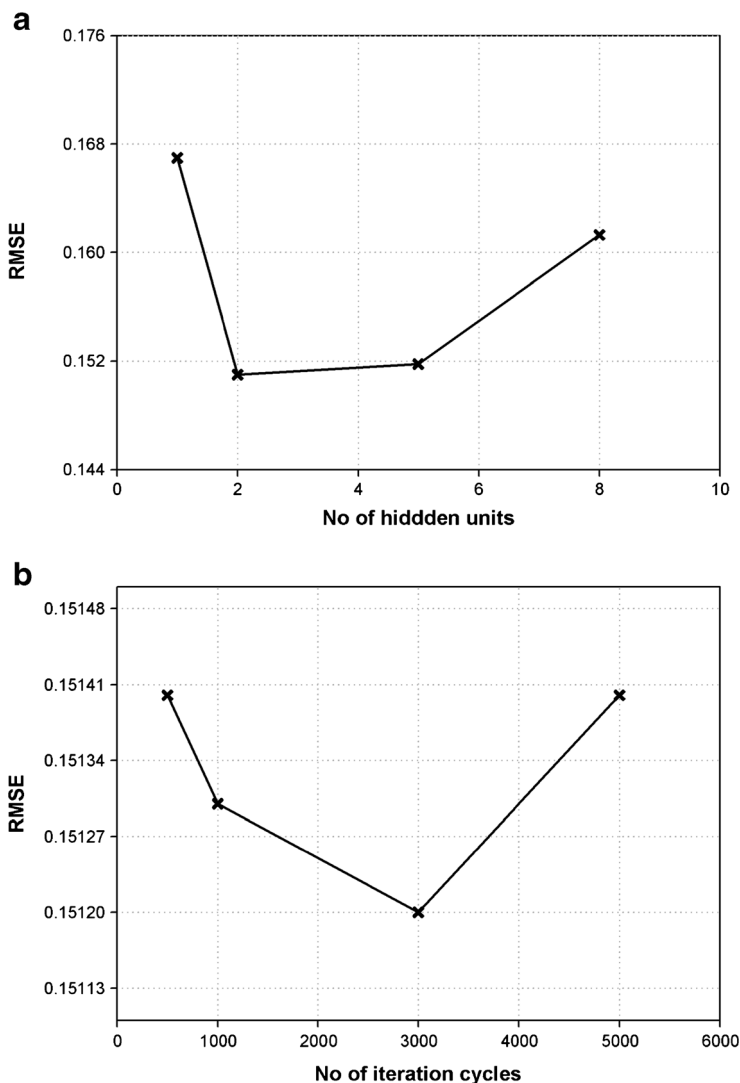


**Fig. VIII.** RMSE values of ANN models during evaluation of optimum hidden units (a) and optimum iteration cycles (b)

ANN structure (shown in Fig. IX) consists of one (1) input layer with two (2) units ( $X_1$  and  $X_2$ ), one (1) hidden layer with four (4) units, and one (1) output layer with two (2) unit ( $Y_{10min}$  and  $Y_{30min}$ ). In addition, optimum number of training iterations was set at 3000, while the average RMSE of correlation for the ANN model was 0.151.

Regarding GP, symbolic regression revealed increased non-linear equations for the correlation between the examined factors and the selected responses. GP is a biologically inspired machine learning method that evolves computer programs to perform a task. When building an empirical mathematical model of data acquired from a process or system, by correlating the independent with dependent variable the process is known as symbolic regression. Unlike traditional regression analysis, symbolic regression automatically evolves both the structure and the parameters of the mathematical model from the data (38). The average RMSE of correlation for the GP symbolic regression equations was 0.273.

Based on the above results, ANN and GP showed increased correlation efficacy compared to MLR with RMSE

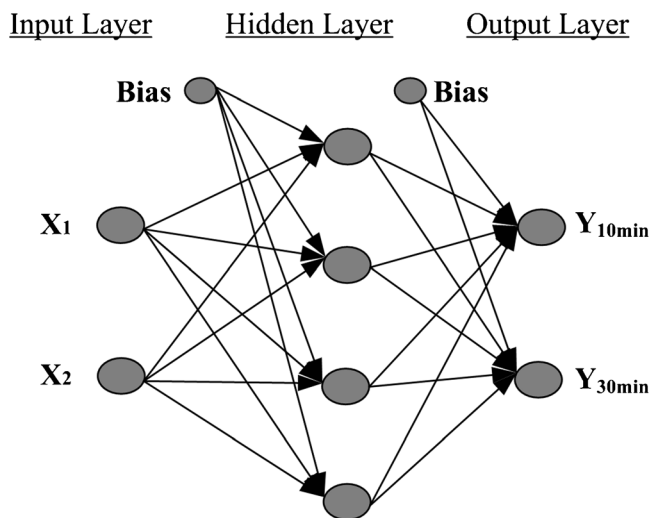


**Fig. IX.** Optimal neural network architecture employing ratio of carrier to coating ( $X_1$ ) and type of solubilizing agent ( $X_2$ ) as input units; and amount of API resealed in 10 min ( $Y_{15min}$ ) and 30 min ( $Y_{30min}$ ) as an output units

of 0.151, 0.273 and 0.413 for ANN, GP and MLR, respectively. This increased correlation efficacy of both ANN and GP can be attributed in their ability to correlate effectively both linear and non-linear multivariate relations, in contrast to MLR where only linear correlation are handled.

## CONCLUSION

The present study showed that liquisolid technique was a successful approach in order to prepare a new aprepitant solid dosage form and to enhance its dissolution rate compared to the marketed product Emend®. Physicochemical characterization of the optimum formulation by means of XRD, SEM, and DLS analyses showed that the increased dissolution rates were due to the formation of API nanocrystals, which, based on stability studies, found to be stable for up to 6 months, while DSC and ATR-FTIR analysis revealed the existence of intermolecular interaction between the API and the excipients used in the liquisolid formulation. Finally, the use of ANNs and GP showed better correlation efficacy when examining the effect of formulation variables on dissolution characteristics compared to MLR.

## ACKNOWLEDGEMENTS

The authors thank Prof. Christos Kontoyiannis of the School of Pharmacy of the University of Patras in Greece for the XRD measurement.

## REFERENCES

- Poli-Bigelli S, Rodrigues-Pereira J, Carides AD, Julie-Ma G, Eldridge K, Hipple A, et al. Addition of the neurokinin 1 receptor antagonist aprepitant to standard antiemetic therapy improves control of chemotherapy-induced nausea and vomiting. Results from a randomized, double-blind, placebo-controlled trial in Latin America. *Cancer*. 2003;97:3090–8.
- European Marketing Authorization, Emend (Aprepitant): Summary of Product Characteristics. 2003. Available at: <https://www.medicines.org.uk/emc/medicine/13868>. Accessed 18 June 2017.
- Wu Y, Loper A, Landis E, Hettrick L, Novak L, Lynn K, et al. The role of biopharmaceutics in the development of a clinical nanoparticle formulation of MK-0869: a Beagle dog model predicts improved bioavailability and diminished food effect on absorption in human. *Int J Pharm*. 2004;285:135–46.
- Singh A, Worku ZA, Van den Mooter G. Oral formulation strategies to improve solubility of poorly water-soluble drugs. *Expert Opin Drug Deliv*. 2011;8:1361–78.
- Kamboj S, Sharma R, Singh K, Rana V. Aprepitant loaded solid preconcentrated microemulsion for enhanced bioavailability: a comparison with micronized aprepitant. *Eur J Pharm Sci*. 2015;78:90–102.
- Kamboj S, Rana V. Formulation optimization of aprepitant microemulsion-loaded silicated corn fiber gum particles for enhanced bioavailability. *Drug Dev Ind Pharm*. 2016;42:1267–82.
- Liu J, Zou M, Piao H, Liu Y, Tang B, Gao Y, et al. Characterization and pharmacokinetic study of aprepitant solid dispersions with soluplus. *Molecules*. 2015;20:11345–56.
- Dhillon R, Ojha R, Bedi N. Preparation, characterization and optimization of poloxamer solid dispersions of a poorly water soluble drug aprepitant. *Br J Pharm Res*. 2014;4:2436–54.
- Rao BC, Vidyadhara S, Sasidhar RLC, Chowdary YA. Dissolution enhancement of poorly soluble drug aprepitant by hot melt extrusion method using hydrophilic polymer: a solid dispersion technique. *Res J Pharm Biol Chem Sci*. 2014;5:1469–85.
- Penumetcha SS, Gutta LN, Dhanala H, Yamili S, Challa S, Rudraraju S, et al. Hot melt extruded Aprepitant-Soluplus solid dispersion: preformulation considerations, stability and in vitro study. *Drug Dev Ind Pharm*. 2016;42:1609–20.
- Sharma R, Kamboj S, Singh G, Rana V. Development of aprepitant loaded orally disintegrating films for enhanced pharmacokinetic performance. *Eur J Pharm Sci*. 2016;84:55–69.
- Ridhurkar DN, Ansari KA, Kumar D, Kaul NS, Krishnamurthy T, Dhawan S, et al. Inclusion complex of aprepitant with cyclodextrin: evaluation of physico-chemical and pharmacokinetic properties. *Drug Dev Ind Pharm*. 2013;39:1783–92.
- Angi R, Solymosi T, Ötvös Z, Ordasi B, Glavinas H, Filipcsei G, et al. Novel continuous flow technology for the development of a nanostructured aprepitant formulation with improved pharmacokinetic properties. *Eur J Pharm Biopharm*. 2014;86:361–8.
- Karavas E, Koutris E, Samara V, Koutri I, Kalaskani A, Kiziridi C, Abatzis M, Bikiaris D, Inventors, Pharmathen S.A., assignee. Pharmaceutical composition comprising aprepitant and method for the preparation thereof. Geneva: World Intellectual Property Organization; 2016.
- Klein S. In vitro lipolysis assay as a prognostic tool for the development of lipid based drug delivery systems (Dissertation). der Martin-Luther-Universität Halle-Wittenberg, Datum der öffentlichen Verteidigung: 30.01.2013.
- Aprepitant scientific discussion, EMEA. 2004. Available at: [https://www.ema.europa.eu/docs/en\\_GB/document\\_library/EPAR\\_-\\_Scientific\\_Discussion/human/000527/WC500026534.pdf](https://www.ema.europa.eu/docs/en_GB/document_library/EPAR_-_Scientific_Discussion/human/000527/WC500026534.pdf). Accessed 20 Feb 2017.
- Spireas S, Bolton S.M. Liquisolid systems and methods of preparing same, US Patent 5968. 1999. p. 550.
- Azharshekoufeh BL, Shokri J, Adibkia K, Javadzadeh Y. Liquisolid technology: what it can do for NSAIDs delivery? *Colloids Surf B Biointerfaces*. 2015;136:185–91.
- Hentzschel CM, Sakmann A, Leopold CS. Suitability of various excipients as carrier and coating materials for liquisolid compacts. *Drug Dev Ind Pharm*. 2011;37:1200–7.
- Singh SK, Srinivasan KK, Gowthamarajan K, Prakash D, Gaikwad NB, Singare DS. Influence of formulation parameters on dissolution rate enhancement of glyburide using liquisolid technique. *Drug Dev Ind Pharm*. 2012;38:961–70.
- El-Hammadi M, Awad N. Investigating the use of liquisolid compacts technique to minimize the influence of pH variations on loratadine release. *AAPS PharmSciTech*. 2012;13(1):53–8.
- Lu M, Xing H, Yang T, Yu J, Yang Z, Sun Y, et al. Dissolution enhancement of tadalafil by liquisolid technique. *Pharm Dev Technol*. 2017;22:77–89.
- Elkordy AA, Tan XN, Essa EA. Spironolactone release from liquisolid formulations prepared with Capryol™90, Solutol® HS-15 and Kollicoat®SR 30D as non-volatile liquid vehicles. *Eur J Pharm Biopharm*. 2013;83:203–23.
- Syed IA, Pavani E. The liquisolid technique: based drug delivery system. *Int J Pharm Sci Drug Res*. 2012;4:88–96.
- Vraníková B, Pavlovská S, Gajdziok J. Experimental design for determination of effects of superdisintegrant combinations on liquisolid system properties. *J Pharm Sci*. 2017;106:817–25.
- Tiong N, Elkordy AA. Effects of liquisolid formulations on dissolution of naproxen. *Eur J Pharm Biopharm*. 2009;73:373–84.
- Javadzadeh Y, Shariati H, Movahhed-Danesh E, Nokhodchi A. Effect of some commercial grades of microcrystalline cellulose on flowability, compressibility, and dissolution profile of piroxicam liquisolid compacts. *Drug Dev Ind Pharm*. 2009;35:243–51.
- Elkadí S, Elsamaligy S, Al-Suwayeh S, Mahmoud H. The Development of self-nanoemulsifying liquisolid tablets to improve the dissolution of simvastatin. *AAPS PharmSciTech*. 2017; <https://doi.org/10.1208/s12249-017-0743-z>.
- Kennard R, Stone L. Computer aided design of experiments. *Technometrics*. 1969;11:137–48.

30. Koza JR. Genetic programming as means for programming computers by natural selection. *Stat Comput.* 1994;4:87–112.
31. Barmpalexis P, Kachrimanis K, Georganakis E. Solid dispersions in the development of a nimodipine floating tablet formulation and optimization by artificial neural networks and genetic programming. *Eur J Pharm Biopharm.* 2011;77:122–31.
32. EPA, United States Environmental Protection Agency. 2014: 2-Pyrrolidone. Available at <http://www.epa.gov/oppt/chemrtk/hpvis/hazchar/16455SN1942-pyrrolidonePOSTpdf>. Assessed 10 Mar 2017.
33. Raghavan SL, Trividic A, Davis AF, Hadgraft J. Crystallization of hydrocortisone acetate: influence of polymers. *Int J Pharm.* 2001;212:213–21.
34. Baird JA, Van Eerdenbrugh B, Taylor LS. A calcification system to assess the crystallization tendency of organic molecules from undercooled melts. *J Pharm Sci.* 2010;99:3787–806.
35. Helmy R, Zhou GX, Chen YW, Crocker L, Wang T, Wenslow RM Jr, et al. Characterization and quantitation of aprepitant drug substance polymorphs by attenuated total reflectance fourier transform infrared spectroscopy. *Anal Chem.* 2003;75(3):605–11.
36. Matsaridou I, Barmpalexis P, Salis A, Nikolakakis I. The influence of surfactant HLB and oil/surfactant ratio on the formation and properties of self-emulsifying pellets and microemulsion reconstitution. *AAPS PharmSciTech.* 2012;13:1319–30.
37. Kabanov AV, Batrakova EV, Alakhov VY. Pluronic block copolymers as novel polymer therapeutics for drug and gene delivery. *J Control Release.* 2002;82:189–212.
38. Searson DP. GPTIPS 2: an open-source software platform for symbolic data mining. Chapter 22. In: Gandomi AH, et al., editors. *Handbook of Genetic Programming Applications*. New York: Springer; 2015.